



TOPOLOGY AND SHAPE OPTIMIZATION OF GEAR CASING USING FINITE ELEMENT AND TAGUCHI BASED STATISTICAL ANALYSES

Jeevanantham A. K. and Pandivelan C.

Department of Manufacturing Engineering, School of Mechanical Engineering, VIT University, Vellore Tamil Nadu, India

E-Mail: akjeevanantham@yahoo.com

ABSTRACT

In this paper, the design optimization of gear casing is performed by reducing the weight and retaining its original stiffness and natural frequencies simultaneously. Through finite element modeling, these multi objectives are achieved in two methods: topology optimization and shape optimization. In first method, displacements and natural frequencies of baseline values are considered as constraints and the optimum weight reduction is analyzed. Later, the dimensional regions to be optimized are identified. With L_9 orthogonal array, the dimensions are varied at these regions by morphing technique, and respective multiple performance characteristics are measured. Taguchi method based grey analysis, which uses grey relational grade as performance index, is specifically adopted to determine the optimal combinations of dimensions. Principal component analysis is applied to evaluate the weights so that their relative significance can be described properly to convert these multiple performance characteristics into a single objective grey relational grade. Confirmation analysis to the optimized design is performed and the resulted frequency and stiffness are compared with baseline values. The results show that grey relational analysis coupled with principal component analysis can effectively acquire the optimal combination of design parameters and the proposed approach can be a useful tool to perform the shape optimization efficiently.

Keywords: topology, shape optimization, finite element analysis, taguchi method, grey relation analysis.

1. INTRODUCTION

The efficient use of materials plays most important role for given design objectives and constraints in a product design process. Significant research efforts have been devoted in sizing, shape and topology optimization to the design of structures and mechanical elements applicable for various aerospace and automotive applications [1]. The goal of sizing may be to find the optimal thickness of a linearly elastic plate. On the other hand the shape optimization is defined on a domain which is the design variable. Topology optimization involves the determination of features and the connectivity of the domain. Shape optimization is closely related to topology optimization, where not only the shape and sizing of a structure has to be found, but also the topology, i.e. the location and shape of features [2].

There are three types of shape optimization problems like parametric shape optimization, traditional (boundary variation) shape optimization, and topology optimization. Each focuses on different aspect of a product design process (in reverse order): conceptual design stage, preliminary design stage and detailed design stage. Parametric shape optimization deals with shape optimization problems in a particular design space in which the shape is parameterized by a finite, and usually small, set of geometric parameters called dimensions. Common examples of dimensions include sizes, radii, distances, angles, and other geometrically meaningful design and/or manufacturing variables. These sets of dimensions are used as design variables which essentially transfer a shape optimization problem into an easy-solving 'sizing' problem. But during this optimization either topology of the shape is fixed or re-parameterization may be required. This method can be easily integrated into computer aided design (CAD) and the resultant parametric

shapes will be manufacturing friendly. In boundary variation shape optimization problems, there is no such high-level geometric parameter. The shape boundary can be moved in any fashion using some parametrization or discretization techniques to generate a set of design variables for the optimization process. Since tracking intersected boundaries is very difficult for parameterized curves/surfaces, this method does not allow topological changes. Much attention has been spent to the topology optimization problems, which focus on how to allow topological changes in the shape optimization process. The importance of topology optimization lies in the fact that the choice of appropriate topology of a structure at the initial design stage is in general the most decisive factor for the efficiency of a product. Among all three optimization problems, topology optimization is the most challenge one mainly due to the lacking of theoretic support [3].

While shape optimization is an iterative multi-objective process, the boundaries among these three aspects should be relaxed as opposed to the current state in shape optimization in order to facilitate design automation. The goal in shape optimization is to find a shape among the set of all admissible shapes that optimizes a given objective function. As such it can be seen as a classical optimization problem where one would like to find a feasible point, i.e. a point that satisfies all constraints, which minimizes a certain cost function [4]. There are various methods that aim to solve shape optimization problems. Existing methods can be divided into three categories: the homogenization method [5] whose physical idea in principle consists of averaging heterogeneous media in order to derive effective properties; the material distribution method [2] where each point in the design can have material or not; and the geometry-based method [3]



in the sense how to move the boundary and where to put the features.

In order to validate the design during initial development stage, various iterations are carried out to bring an optimal one. Recent advances in commercial codes for producing optimal design has shortened the iterative process and eliminated the trial and error method. The design cycle almost always originates with a concept drawing and ends as a manufacturing drawing. This is the major problem how to translate a sketch into an acceptable design for manufacturing. A typical design cycle involves numerous trades-offs, like appearance versus function, cost versus ease of manufacture, etc. The widespread use of 3D CAD software has made it easier for engineers to recreate manufacturing drawings when the design changes. The advancement of technology has changed the way in which the design cycle has been addressed. The latest method is not to validate the benchmark design using computer aided engineering (CAE) but the commercial finite element codes to give an optimal design for the given loading conditions. Conceptual design tools such as topology optimization can be introduced to enhance the design process. Topology optimization provides a new design boundary and optimal material distribution. The resulting design space is given back to the designer, where the suitable modifications are done using CAD software. The optimized design will always be lighter and usually stiffer than the concept design. Optimization techniques have been used widely in various applications including structural design [6]. The cycle time and cost of making prototypes in an iterative design process is high. Hence it is important to make maximum use of computer aided simulation tools, upfront in the design process, such that the product can be designed right at the first time [7]. The topology optimization method has been applied to various areas, including structural design and material design for desired Eigen frequencies [8], [9], [10], [11] and other dynamic response characteristics [12]. With the current technology the users have to first do a topology optimization and get an approximate model of the structure under a given loading. Later, the size and shape must be optimized to find out the required dimensions of the structure to support the loading [13]. The Large Admissible Perturbation (LEAP) theory has solved various redesign problems without trial and error or repetitive finite element analyses.

In general, shape and topology optimization problems are solved using repeated runs of finite element analysis. Structural performance constraints such as static deflections and natural frequencies are used instead of volume or material density as constraints. Topology optimization has received extensive attention since an epoch-making paper published by Bendsoe and Kikuchi [14]. They developed the method of homogenization for topology and shape optimization. Both optimization problems have been studied extensively from then on [15]. These optimizations are the most recent method to become available and hold the most promise for designing castings, moldings, and other parts which must be modeled with solid elements [16].

A normal modes analysis can be used to guide the experiment. In the pretest planning stages, it can be used to indicate the best location of the accelerometers. It is also useful to correlate the test results with finite element investigation. Correlation is necessary to validate the CAE method and apply it confidently for design iterations and improve the designs through optimization techniques, so that these virtual iterations will work in the field as well. An overall understanding of normal mode analysis as well as knowledge of the natural frequencies and mode shapes for a particular structure is important for all types of dynamic analysis. For the low frequency range, the finite element method (FEM) and the boundary element method (BEM) are still most widely used in the dynamic analysis [17]. However, FEM and BEM become computationally expensive or even impractical, and they are also sensitive to changes in boundary conditions at high frequency. Statistical energy for predicting average response at high frequency analysis is the most widely used energy-based method. As an alternative method to Statistical Energy Analysis (SEA), an emerging method for high frequency simulations is the Energy Finite Element Analysis (EFEA) [18]. SEA has been an accepted and effective analysis tool for high-frequency acoustics and vibration analysis since the 1960's [19]. Modal Analysis is an accepted tool in advanced mechanical engineering to estimate the modal parameters without known input forces [20]. Frequency response analysis are experimentally performed to curve fit the experimental modal properties like natural frequencies, mode shapes and damping [21]. These results are validated using results obtained in CAE. But recent trends in automotive development activities for reduction of lead-time and cost have led to use CAE techniques by skipping conventional development steps of making and checking costly prototypes. In frequency response analysis the excitation is explicitly defined in the frequency domain. It gives good insight of high stress region and used for comparative design evaluation when the measured data does not available [22].

This paper focuses the parametric shape optimization of gearbox casing. It is the shell (metal casing) in which a train of gears is sealed. By the rotation of the gears, vibrations are developed in gearbox casing. The torque generated in the engines is transmitted to the shafts and gears. The reaction force that is generated by the gears is transmitted to bearings which support the shafts to the casing as bearing load [23]. The housing surface emits the sound which penetrates from the inner space through the walls, as well as the sound generated by the housing with its natural oscillation. From this aspect, the housing walls have a double role: to be an obstacle to the penetration of sound waves from the inside, i.e. to be the insulator of inner (internal) sound sources and the generator of tertiary sound waves due to natural oscillation [24]. The rib stiffener layout is the key to the design, and the most effective position of stiffeners for reducing the vibration must be sought, though several studies have been reported on the layout design [25]. The goal in this parametric shape optimization is to reduce the weight of gear casing but indeed the multiple targets of increased



natural frequency and displacements, and reduced volume with the constraint of fixed topology at several design spaces. This parametric shape optimization is planned to achieve the multiple objectives using Taguchi method based grey relational analysis (GRA) coupled with principal component analysis (PCA) [26].

2. PROPOSED METHODOLOGY

FEM of the gear casing is developed using finite element software 'SimLab' with Tetra 10 elements. The loads and boundary conditions are imposed on the gear casing to carry out the linear static and modal analysis. The baseline design is thoroughly studied by these analyses. At the same time these baseline frequencies are validated by the modal based frequency response analysis and modal analysis in two different solvers: ABAQUS and NASTRAN. The validated baseline results are set as constraints to perform the topology optimization at various iterations. By fixing the design from topology optimization, the parametric shape optimization is performed. Here, five different regions are identified in the gear casing based on where the material was optimized during topology optimization. Based on the required degrees of freedom for the five design (shape) parameters each at two dimensional levels, the suitable orthogonal array is selected for the Taguchi's experimental analysis. The multiple performance characteristics (responses/objectives) are selected for the efficient design optimization. The dimensions of five design parameters are varied according to the levels in the orthogonal array using morphing technique called 'Hypermorph' option in the optimization software OptiStruct. Thus Taguchi's experimentation is conducted and the corresponding performance characteristics are noted using FEM.

The multiple performance characteristics are preprocessed so that these original values can be normalized in the range of 0 and 1 based on the respective category of multi objective (maximization, minimization or normalization). Following the preprocessing, a grey coefficient is calculated to express the relationship between the ideal and actual normalized performance characteristics. Actually the grey relational grade for each experiment has to be calculated by averaging their grey coefficients. In this multivariate analysis, the information from the multiple grey coefficients may overlaps due to their variations and internal correlation to some extent. PCA is applied to simplify this issue by dimension reduction to find the uncorrelated compositive factors that reflect original information as much as possible to represent the entire original multiple characteristics. The grey relational coefficients are used to evaluate the correlation coefficient matrix and to determine the corresponding eigenvalues. From the eigenvalue larger than one, the principal component information is extracted. Thus the correlated grey coefficients are transformed into a set of uncorrelated weighted components for each performance characteristics. By considering the weighting values to each performance characteristics in grey coefficients, the multi-objective

performance characteristics are converted into single objective grey relational grade for each experimental runs. The grey relational grade represents the level of correlation between the sequences of multi performance characteristics and the experimental run. If the two sequences are identical, then the value of grey relational grade is equal to one. The gray relational grade also indicates the degree of influence that sequence of experimental runs could exert over the sequence of multi performance characteristics. Therefore, if a particular experimental run is more important than other runs to the sequence of performance characteristics, then the grey relational grade for that experimental run and its performance characteristics will be higher than other grey relational grades. So the dimensional settings of the design parameters at the experimental run with highest grey relational grade are considered as optimum one. From the inferences of plot for main effects, the best combination of dimensional levels of design parameters is chosen in turn correlated with topology optimization. Confirmation analysis to this optimized design is performed using FEA and the resulted frequency and stiffness are compared with baseline values.

3. FINITE ELEMENT MODELLING OF GEAR CASING

The three-dimensional solid model of the gear casing is developed with UG software. It is further imported into the finite element software 'SimLab' using TETRA mesh of size 10 mm. There are totally 107121 tetra10 elements and 183005 nodes in the meshed model.

3.1 Boundary conditions and material properties

The engine torque is transmitted to shaft and gears fixed in the housing. The modified torque is transmitted then to the drive shaft. For modal analysis the power train mounts are constrained in all translations and rotation. The gear casing is bolted to the engine head. The bolted connections are represented by rigid body elements to constrain the bolt holes (mounts) of the gear casing [25]. The commonly used material for gear casing is Aluminum and Cast Iron. Since cast iron is practiced in most applications, its material properties like 1.69×10^5 MPa of Young's modulus 'E', 0.257 of Poisson ratio ' μ ' and 7006 Kg/m³ of Density ' ρ ' are considered for this analysis.

3.2 Natural frequencies and mode shapes

The normal mode analysis is performed for the gear casing using RADIOSS linear solver. The first ten natural frequencies and their corresponding mode shapes are extracted using normal mode analysis. To validate the natural frequencies, two other solvers ABAQUS and MSC NASTRAN are utilized to check whether the natural frequencies are close to each other. They are compared and validated as shown in Table-1.



Table-1. Natural frequency comparison for gear casing in three different solvers.

Modes	Natural frequency (Hz)		
	RADIOSS	NASTRAN	ABAQUS
1	996	997	997
2	1150	1152	1150
3	1230	1236	1237
4	1420	1429	1427
5	1670	1672	1674
6	1720	1724	1731
7	1730	1744	1754
8	1870	1889	1879
9	1910	1917	1921
10	1990	1998	1995

3.3 Dynamic analysis

The dynamic analysis of the gear casing is carried by performing the steps in the order of normal mode analysis and forced response analysis. The solution process reflects the nature of the applied dynamic loading. The results of a forced response analysis are evaluated in terms of the system design. In this paper, since the modal analysis is performed as the first step, only forced response analysis is considered for the dynamic analysis.

Frequency response analysis is a method to find the response of a structure subjected to frequency dependent loading. It can be determined by two methods namely: direct frequency response and modal frequency response analysis. The direct method calculates the response directly in terms of the physical degrees of freedom in the model. The modal method calculates the response based on the eigenvalues and eigenvectors obtained from normal mode analysis. The modal method is computationally cheaper than the direct method. In this paper, SimLab is used for the analysis of modal frequency response. It needs a normal mode analysis result file to proceed with the frequency response analysis. So NASTRAN normal mode analysis results file is prepared for the analysis on SimLab.

3.3.1 Frequency response analysis

The response of the gear casing can be reproduced by applying generalized forces to empty housing. This bearing load causes the transmission housing to deform. An important aspect of a frequency response analysis is the definition of the loading function. In a frequency response analysis, the force must be defined as a function of frequency. In the same manner forces are applied here. There are two important aspects of dynamic load definition. First, the location of the loading on the structure must be defined. Since this characteristic locates the loading in space, it is called the spatial distribution of the dynamic loading. Next the frequency variation in the loading is the characteristic that

differentiates a dynamic load from a static load. This frequency variation is called the temporal distribution of the load. A complete dynamic loading is a product of spatial and temporal distributions. Another important aspect of frequency response analysis is selecting the frequency at which the solution is to be performed. Undamped or very lightly damped structures exhibit large dynamic responses for excitation frequencies near resonant frequencies. For maximum efficiency, an uneven frequency step size should be used. Smaller frequency spacing should be used in regions near the resonant frequencies, and larger frequency step sizes should be used in regions away from resonant frequencies.

3.3.2 Input values for the frequency response analysis

In order to excite modal oscillation, it is not always enough to move the system out of the equilibrium state and in the direction of the greatest deformations. Sometimes it is necessary to realize excitation with a frequency which is equal to the natural frequency of the modal shape that should be excited. So, the deformation or the force should be changed with the same frequency. For determination of response by direct integration of the finite element structure, it is suitable to use sine excitation functions whose frequencies are equal to the frequencies of modal shapes and whose response is determined. The frequency of excitation force should be varied so that it coincides with modal frequencies. Thus the response of the system for corresponding frequencies depending on the point of force action is obtained.

A frequency response analysis is performed on excitation frequency range of 850 - 2000 Hz. A sinusoidal unit load of 1N is applied on the bearing region at the node ID 95590. The resulting file (*.csv) gives the nodal displacement at each frequency. At these input values the resultant frequency curves are shown in Figure-1. It shows the response by the system for sinusoidal input that the peak displacement for unit load is equal to 2.189×10^{-3} mm. The peak displacement is obtained at an excitation frequency close to first resonant frequency. This curve also shows the peak displacement at other resonant frequencies. In conclusion, it is known that the generalized forces transmitted to the bearings on empty casing allow us to simulate the response of the casing.

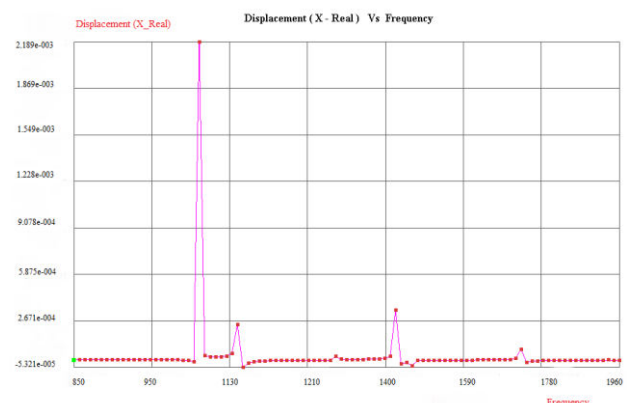


Figure-1. Frequency response curve for the gear casing.



3.4. Linear static analysis

The loading conditions are imposed on the gear casing such that the stiffness of the gear casing can be determined. Four bearing surfaces: Bearing surfaces 1 (BTM), 2 (TOP1), 3 (TOP2) and 4 (TOP3) are selected as shown in Figure-2. To maintain the stiffness at every region of the casing, loads are applied at every bearing surface in six different directions: Forces at X direction (FX), Y direction (FY) and Z direction (FZ), and the moments at X direction (MX), Y direction (MY) and Z direction (MZ). Since there are four bearing surfaces, 24 load cases are applied on the gear casing to perform the linear static analysis. When a force is applied to a spring mass system, the displacement produced can be calculated. Then the stiffness is made based on the governing Eq. (1).

$$k = \frac{f}{\delta} \quad (1)$$

where,

k = stiffness (N/mm); f = force applied (N); δ = deflection (mm)

The boundary conditions are applied before performing the linear static analysis. Figure-2 shows the loading conditions such that the stiffness of the system can be taken to the deflection produced by 10,000 N load applied on the body. The contour plots for all load cases are saved and respective displacements are calculated for each 24 load cases as shown in Table-2.

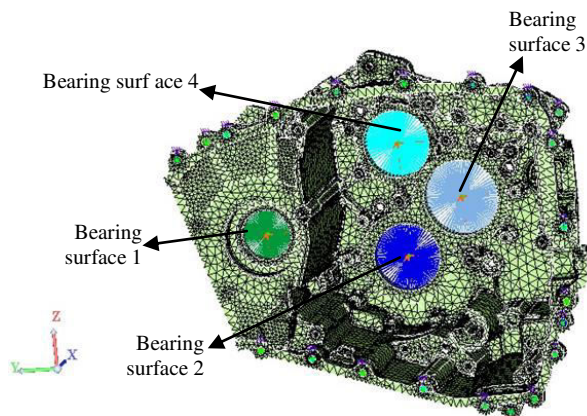


Figure-2. Finite element model of gear casing with boundary conditions applied.

Table-2. Displacements for all the load cases applied on the gear casing.

Load case	Bearing region	Displacement (mm) (Baseline values)
1	F _X BTM	0.091
2	F _Y BTM	0.0378
3	F _Z BTM	0.0169
4	M _X BTM	0.000259
5	M _Y BTM	0.000625
6	M _Z BTM	0.00215
7	F _X TOP1	0.113
8	F _Y TOP1	0.0377
9	F _Z TOP1	0.0351
10	M _X TOP1	0.000221
11	M _Y TOP1	0.00153
12	M _Z TOP1	0.00259
13	F _X TOP2	0.203
14	F _Y TOP2	0.0369
15	F _Z TOP2	0.0446
16	M _X TOP2	0.000219
17	M _Y TOP2	0.00185
18	M _Z TOP2	0.00262
19	F _X TOP3	0.0823
20	F _Y TOP3	0.0312
21	F _Z TOP3	0.035
22	M _X TOP3	0.000229
23	M _Y TOP3	0.0013
24	M _Z TOP3	0.00105

4. DESIGN OPTIMIZATION OF GEAR CASING

In this paper, the design optimization of the gear casing is performed in two ways: topology optimization and shape optimization, using the optimization software OptiStruct. For the significant weight reduction or complete redesign, topology optimization is used. To efficiently modify the design so as to add new features like fillets, ribs, bolt holes, shape optimization is performed.

4.1 Topology optimization

Topological optimization has been developed to make the design stage easier and to find new design concepts. Development of a new component is based on the topology used in a similar case in the past. The primary importance of keeping the knowledge about the original design can be easily maintained. The weight reduction in the gear casing is attained by retaining the natural frequencies and the stiffness of the material. The baseline design values obtained by normal mode analysis and linear static analysis at previous section are kept as



design constraints to perform the topology optimization. The material distributions for the given set of loading conditions are analyzed during the topology optimization. The main aspect of getting right result while performing topology optimization is to give right input data so that the solver results a feasible solution. More numbers of design constraints may lead the solver to an infeasible design. So the first three baseline natural frequencies 996, 1150 and 1230 Hz (shown in Table-1) are considered as design constraints out of ten natural frequencies. The design space for topology optimization is identified through intuition and trial & error. In this analysis, the bearing surface and the mounts of the gear casing are considered as non-design space, and rest of the region is considered as design space. Since the gear casing is already an optimized design, the solver requires some amount of material to carry out the topology optimization. So material is added at design spaces in case the analyst wants to redesign. The more material is added the optimizer has the ability to give more accurate results.

The optimization can be achieved only by either compromising the displacement and natural frequencies or varying both in order to obtain an optimal design. The design constraints are varied based on increase of percentage from 1 to 5% for displacement and natural frequencies from 5 to 20 % from original values. Totally 20 experiments are conducted and checked for weight reduction in the gear casing. Table 3 shows the volume of gear casing for each combination of varying frequencies and displacements where the initial volume of the gear casing is $2.44 \times 10^6 \text{ mm}^3$.

Table-3. Design parameters and their levels (mm) for the gear casing experimental design.

Design parameters	Original design	Level 1	Level 2
Fbr	3.106	2.950	2.795
F	6.993	6.643	6.29
Bh	4.498	4.273	4.059
Bc	7.5	7.125	6.75
Wt	27.81	26.4195	25.029

Even though there is significant weight reduction, the results shown have no significant change in the natural frequencies due to the change in design constraints (natural frequencies) from 5 to 20%. Since the displacement is considered as the significant effect for weight reduction, the extreme case with 5% displacement and 20% natural frequency is chosen as they yield maximum (11.88%) weight reduction of all the trials. The topology optimized design is shown in Figure-3.

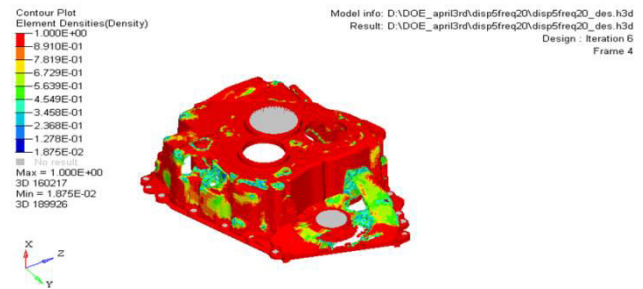


Figure-3. Topology optimized gear casing design by OptiStruct.

Though the solver has given optimized results, the optimized design is regenerated for being in safer side. Linear static analysis and normal mode analysis are performed. The displacement and natural frequency values are compared with the baseline. The percentage change in the weight of gear casing is 11.88 %. This volume is imported back into CAD to get a lighter weight casing retaining the stiffness and natural frequencies closer to the original design.

4.2 Multi objective shape optimization

In this paper, the shape optimization is performed using Taguchi's parameter design where the experimental design approach is used to determine the optimal dimensions of the design parameters of gear casing. Moreover an objective of reduction in weight of gear casing is achieved by retaining the other objectives called maximizing the natural frequencies and displacements. The use of grey based Taguchi method coupled with principal component analysis for this multi-objective optimization with multiple design parameters includes the following steps:

- Identify the regions (design parameters) of gear casing.
- Determine the dimensional range (levels) for each design parameter.
- Select an appropriate orthogonal array and assign the design parameters to its columns.
- Conduct the experiments and note down the multiple performance characteristics (responses).
- Calculate the S/N ratios to the respective responses.
- Normalize the S/N ratios.
- Perform the grey relational generating and calculate the grey relational coefficient.
- Use PCA to calculate the grey relational grades.
- Construct plot for main effects using grey relational grade.
- Choose the optimal dimensional levels of design parameters.
- Verify the displacements and natural frequency of shape optimized design through the confirmation analysis.

The dimensional regions, in which the material had been removed during topology optimization, are chosen for the shape optimization. The areas of fillet at



bearing region, fillets, bolt holes, bolt cover and wall thickness shown in Figure-4 are selected as design parameters. Each design parameters are considered with two dimensional levels: first level is reduced by 5% and second level by 10% from the original dimensions as tabulated in Table-4. The shapes of the fillet sizes are reduced using Morphing technique called “Hypermorph” in OptiStruct.

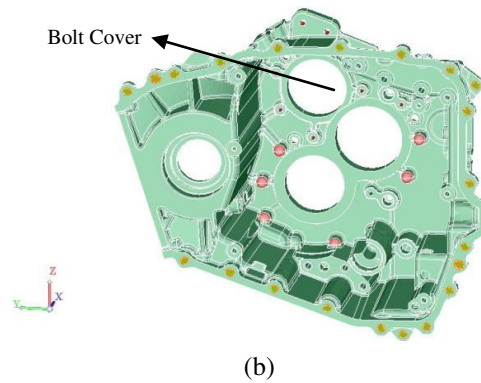
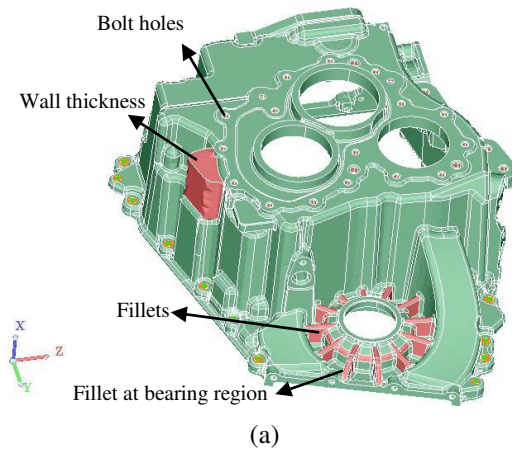


Figure-4. Regions of the design parameters.

Since five numbers of total degrees of freedom is required for this analysis having five parameters each at two levels, L_8 orthogonal array is selected. The multiple performance characteristics (volume, frequency and displacement) at each experimental setting are measured and tabulated as shown in Table-4.

Table-4. Experimental layout of L_8 orthogonal array.

Exp No.	Design parameters and their levels (mm)					Responses		
	Fbr	F	Bh	Bc	Wt	Vol (mm ³)	Freq (Hz)	Disp (mm)
1	2.9507	6.64	4.273	7.125	26.4195	2431000	1009	0.092
2	2.9507	6.64	4.273	6.75	25.029	2429000	1016	0.093
3	2.9507	6.29	4.059	7.125	26.4195	2432000	1026	0.091
4	2.9507	6.29	4.059	6.75	25.029	2428000	1005	0.094
5	2.7954	6.64	4.059	7.125	25.029	2429000	1019	0.094
6	2.7954	6.64	4.059	6.75	26.4195	2426950	1014	0.093
7	2.7954	6.29	4.273	7.125	25.029	2428700	1008	0.093
8	2.7954	6.29	4.273	6.75	26.4195	2426500	1021	0.092

4.2.1 Signal-to-noise ratio

Since the usage of S/N ratios called smaller the better (η_{STB}), higher the better (η_{HTB}) and nominal the better (η_{NTB}) are recommended to measure the performance characteristics deviating from the desired values, weight reduction is considered as a smaller the better case, natural frequency and displacement are considered as a higher the better case. The S/N ratio with a smaller-the-better performance characteristic can be expressed as

$$\eta_{ij(STB)} = -10 \log \left(\frac{1}{n} \sum_{j=1}^n y_{ij}^2 \right) \quad (2)$$

The S/N ratio with a higher-the-better performance characteristic can be expressed as

$$\eta_{ij(HTB)} = -10 \log \left(\frac{1}{n} \sum_{j=1}^n \frac{1}{y_{ij}^2} \right) \quad (3)$$

The S/N ratio with a nominal-the-better performance characteristic can be expressed as

$$\eta_{ij(NTB)} = 10 \log \left(\frac{1}{ns} \sum_{j=1}^n y_{ij}^2 \right) \quad (4)$$

Where η_{ij} is the j^{th} S/N ratio of the i^{th} experiment, y_{ij} is the i^{th} experiment at the j^{th} test, n is the total number of the tests, and s is the standard deviation. Using the Eqs. (2) and (3), the S/N ratios for the respective observations are calculated and shown in Table-5.

**Table-5.** S/N ratios of the observations.

Runs	Original sequence		
	η_{STB} (Volume)	η_{HTB} (Frequency)	η_{HTB} (Displacement)
1	-127.71570	60.07782	-20.72424
2	-127.70855	60.13787	-20.63034
3	-127.71927	60.22295	-20.81917
4	-127.70497	60.04332	-20.53744
5	-127.70855	60.16348	-20.53744
6	-127.70122	60.12076	-20.63034
7	-127.70748	60.06921	-20.63034
8	-127.69961	60.18051	-20.72424

4.2.2 Grey relational analysis

In grey relational analysis, the function of different factors is neglected in situations where the range of the sequence is large. This avoids the problem of different scales, units, and targets. However, this analysis might produce incorrect results, if the factors, goals, and directions are different. A linear normalization of the S/N ratios of responses is performed in the range between 0 and 1, which is called as the grey relational generating. The procedure of grey relation analysis is described as follows.

4.2.2.1. Data preprocessing

The first step called data preprocessing transfers the original sequence to a comparable sequence. For this purpose, S/N ratios are normalized in the range between 0 and 1. The normalization can be done from three different approaches:

If the expectancy is smaller-the-better, then the original sequence should be normalized as follows:

$$X_i^*(k) = \frac{\max X_i^0(k) - X_i^0(k)}{\max X_i^0(k) - \min X_i^0(k)} \quad (5)$$

If the target value of original sequence is infinite, then it has a characteristic of higher-the-better. Then the original sequence can be normalized as follows:

$$X_i^*(k) = \frac{X_i^0(k) - \min X_i^0(k)}{\max X_i^0(k) - \min X_i^0(k)} \quad (6)$$

However, if there is a definite target value to be achieved, the original sequence will be normalized in the form

$$X_i^*(k) = 1 - \frac{|X_i^0(k) - X^0|}{\max \{ \max X_i^0(k) - X^0, X^0 - \max X_i^0(k) \}} \quad (7)$$

or the original sequence can be simply normalized by the most basic methodology, i.e., let the values of original sequence be divided by the first value of sequence

$$X_i^*(k) = \frac{X_i^0(k)}{X_i^0(1)} \quad (8)$$

Where $X_i^0(k)$ is the value after the grey relational generation (data preprocessing), $\max X_i^0(k)$ is the largest value of $X_i^0(k)$, $\min X_i^0(k)$ is the smallest value of $X_i^0(k)$ and X^0 is the desired value.

The S/N ratios of volume, frequency and displacement are set to be the reference sequence $X_i^0(k), k=1-3$. The results of eight experiments are the comparability sequences $X_i^*(k), i=1,2,3,8, k=1-3$. Since higher values of S/N ratios are preferable in the parameter design, all the sequences following data preprocessing are calculated using the Eq. (5).

4.2.2.2. Grey relational coefficient

Following the data preprocessing, a grey relational coefficient is calculated to express the relationship between the ideal and actual normalized experimental results. The grey relational coefficient $\xi_i(k)$ can be expressed as follows:

$$\xi_i(k) = \frac{\Delta \min + \zeta \cdot \Delta \max}{\Delta_{0i}(k) + \zeta \cdot \Delta \max} \quad (9)$$

where $\Delta_{0i}(k)$ called the deviation sequence, is the absolute value between the reference sequence $X_0^*(k)$ and comparability sequence $X_i^*(k)$ namely

$$\Delta_{0i}(k) = \|X_0^*(k) - X_i^*(k)\|$$

$$\Delta_{\max} = \max_{\forall j \in i} \max_{\forall k} \|X_0^*(k) - X_j^*(k)\|$$

$$\Delta_{\min} = \min_{\forall j \in i} \min_{\forall k} \|X_0^*(k) - X_j^*(k)\|$$

The deviation sequences $\Delta_{0i}, \Delta_{\max}(k)$ and $\Delta_{\min}(k)$ for $i=1-8$ and $k=1-3$ are calculated. ζ is distinguishing or identification coefficient: $\zeta \in [0,1]$, since all the design parameters are given with equal importance, generally used value of $\zeta = 0.5$ is substituted in Eq. (9). Table-6 lists the grey relational coefficient for each observations of L_8 orthogonal array.

**Table-6.** Grey relation coefficient.

Exp No.	Grey relational coefficient $\xi_i(k)$		
	Volume	Frequency	Displacement
1	0.37926	0.38229	0.42990
2	0.52366	0.51355	0.60260
3	0.33333	1.00000	0.33333
4	0.64687	0.33333	1.00000
5	0.52366	0.60166	1.00000
6	0.85925	0.46777	0.60260
7	0.55539	0.36877	0.60260
8	1.00000	0.67914	0.42990

After obtaining the grey relational coefficient, its average has to be calculated to obtain the grey relational grade. The grey relational grade is defined as follows

$$\gamma_i = \frac{1}{n} \sum_{k=1}^n \xi_i(k) \quad (10)$$

However, since in real applications the effect of each parameter on the product is not exactly same, the above equation can be modified as a weighted average of grey coefficients of multi objectives. It is determined using Eq. (11) as

$$\gamma_i = \sum_{k=1}^n w_k \xi_i(k) \quad \text{where,} \quad \sum_{k=1}^n w_k = 1 \quad (11)$$

where w_k represents the normalized weighting value of factor k . If the two sequences are identical, then the value of grey relational grade is equal to 1. Given the same weights, the Eqs. (10) and (11) are equal.

4.2.2.3. Grey relational grade

In GRA, the grey relational grade is used to show the relationship among the sequences. It also indicates the degree of influence that the comparability sequence could exert over the reference sequence. Therefore, if a particular comparability sequence is more important than the other comparability sequence to the reference sequence, then the grey relational grade for that comparability sequence and reference sequence will be higher than other grey relational grades. In this paper, the corresponding weighting values, i.e., w_k for each performance characteristics (i.e., responses) are obtained from PCA to reflect their relative importance in the GRA.

4.2.3. Principal component analysis

PCA is a useful statistical method to convert multi-indicators to several compositive ones. This approach explains the structure of variance-covariance by way of the linear combinations of each performance

characteristic. The procedure of PCA using covariance matrix is described as follows:

4.2.3.1. The original multiple performance characteristic array

$x_i(j)$, $i = 1, 2, \dots, m$; $j = 1, 2, \dots, n$

$$X = \begin{bmatrix} x_1(1) & x_1(2) & \dots & x_1(n) \\ x_2(1) & x_2(2) & \dots & x_2(n) \\ \vdots & \vdots & \ddots & \vdots \\ x_m(1) & x_m(2) & \dots & x_m(n) \end{bmatrix} \quad (12)$$

where m is the number of experiment, n is the number of the response variables and x is the grey relational coefficient of each response variable. In this paper, original multiple performance characteristic array is obtained from the Table 7 with the size of $m=8$ and $n=3$.

4.2.3.2. Correlation coefficient array

The correlation coefficient array is evaluated as follows:

$$R_{jl} = \left(\frac{\text{Cov}(x_i(j), x_i(l))}{\sigma_{x_i(j)} \times \sigma_{x_i(l)}} \right), \quad j = 1, 2, 3, \dots, n; \quad l = 1, 2, 3, \dots, n \quad (13)$$

where, $\text{Cov}(x_i(j), x_i(l))$ is the covariance of sequences $x_i(j)$, $x_i(l)$ and $\sigma_i(j)$, $\sigma_i(l)$ are the standard deviation of sequences $x_i(j)$ and $x_i(l)$ respectively. The correlation coefficient array for the multiple performance characteristic array of Table-7 is shown in Eq.14.

$$R_{3 \times 3} = \begin{bmatrix} 1.00000 & -0.15925 & 0.07138 \\ -0.15925 & 1.00000 & -0.46212 \\ 0.07138 & -0.46212 & 1.00000 \end{bmatrix} \quad (14)$$

4.2.3.3. Determining the eigen values and eigenvectors

The eigen values and eigenvectors are determined from the correlation coefficient array,

$$(R - \lambda_k I_m) V_{ik} = 0 \quad (15)$$

where λ_k eigen values $\sum_{k=1}^n \lambda_k = n, k = 1, 2, \dots, n$.

$V_{ik} = [a_{k1} a_{k2} \dots a_{kn}]^T$ eigenvectors corresponding to the eigen value λ_k . The eigen values and corresponding eigenvectors listed in Tables 8 and 9 separately which are acquired using Eq. (15).

4.2.3.4. Principal components

The uncorrelated principal component is formulated as:

$$Y_{mk} = \sum_{i=1}^n X_m(i) \cdot V_{ik} \quad (16)$$



Where Y_{m1} is called the first principal component, Y_{m2} is called the second principal component, and so on. The principal components are aligned in descending order with respect to variance, and therefore, the first principal component Y_{m1} accounts for most variance in the data. The square of the eigenvalue matrix represents the contribution of the respective performance characteristic to the principal component. As explained in Table-7, it is understood that the variance contribution of first principal component characterizes as high as 50.5%. So, From Table-8 it is calculated that the variance contribution of volume, frequency and displacement for

the principal component are 1.09892, -2.48051 and 2.38159 respectively.

Table-7. Eigen values and explained variation for principal components.

Principal components	Eigen value	Explained variation (%)
First	1.51420	50.5
Second	0.9566	31.9
Third	0.5292	17.6

Table-8. Eigenvectors for principal components.

Response variables	Eigenvector		
	First principal component	Second principal component	Third principal component
Volume	0.3044	0.9423	0.1391
Frequency	-0.6871	0.1161	0.7172
Displacement	0.6597	-0.3138	0.6828

4.2.4 Grey relational grade coupled with PCA

In this paper, the weights of the three performance characteristics w_1, w_2 and w_3 are set as 1.09892, -2.48051 and 2.38159 respectively. Based on Eq. (11), the grey relational grade of the comparability sequences $i=1-8$ for the grey relational coefficients $\xi_i(k)$ where $k=1-3$ shown in Table 7, are calculated and shown in Fig. 5. For example, the grey relational grade of the first comparability sequence ($i=1$) is calculated as follows:
 $\gamma_1 = (0.37926 \times 1.09892) + (0.38229 \times -2.48051) + (0.4299 \times 2.38159) = 0.49237$
 Thus, the shape optimization is desirably performed with respect to a single grey relational grade rather than complicated multi objectives. It is clearly observed from Fig. 5 that the levels of design parameter at third experiment has the highest grey relational grade. So, the third experiment gives the best multi-performance characteristics among the eight experiments.

Taguchi's L_8 orthogonal array shown in Table-5 is employed here to analyze the impact for each dimensional level of design parameter by considering the grey relational grade as a response in respective experimental run. Plot for main effects is constructed by sorting the grey relational grades corresponding to levels of the design parameter in each column of the orthogonal array, taking an average on those with the same level. The average grey relational grades in each dimensional level of design parameter 'Fillet at bearing region' are calculated as follows:

$$\text{Fillet at bearing region } (2.9507\text{mm}) = \frac{0.49237 + 0.73672 - 1.32034 + 2.26561}{4} = 0.54359$$

$$\text{Fillet at bearing region } (2.7954\text{mm}) = \frac{1.46463 + 1.21907 + 1.13073 + 0.43816}{4} = 1.06315$$

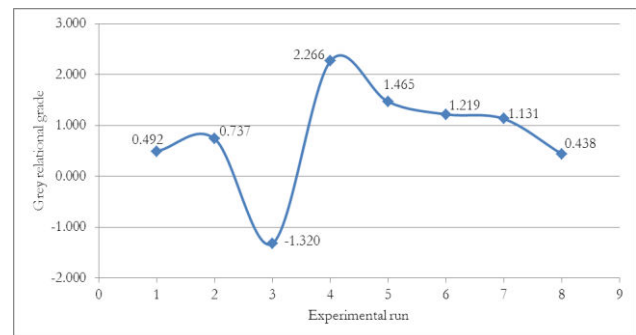


Figure-5. Graph for grey relational grade.

The average of corresponding grey relational grade for individual dimensional level of each design parameter is calculated and shown in Table-10 and Figure-6. Basically, the larger the grey relational grade, the better is the multiple performance characteristics. Thus the optimal dimensional levels (2-1-2-2-2) of each design parameter marked with "*" in Table-10 are the fillet at bearing region at level 2, fillets at level 1, bolt holes at level 2, bolt cover at level 2 and wall thickness at level 2. The influence of each design parameters can be more clearly presented by the means of grey relational grade graph shown in Figure-6. Furthermore, the main effects Table 10 indicates that the wall thickness has the highest level difference (max-min) value of grey relational grade 1.19211 followed by bolt cover, fillet at bearing region, fillets and bolt holes. This indicates that the wall thickness has maximum influence effect on multi-objective characteristics followed by the same sequence. Though the experiment no. 4 at the level sequence of 1-2-2-2-2 is resulted with high grey relational grade, the outcome of main effects as shown in Table-9 and Figure-6 confirms the best combination of levels as 2-1-2-2-2. Therefore the optimum product parameters for this multi objective



criterion are 2.7954 mm of fillet at bearing region, 6.64 mm of fillets, 4.059 mm of bolt holes, 6.75 mm of bolt cover and 25.029 mm of wall thickness (as shown in Table

10) is the best combination to make the multi objectives of reduced volume, increased frequency and normalized displacement in the gear casing design.

Table-9. Main effects through grey relational grade.

Design parameters	Levels		Range	Order
	1	2		
Fillet at bearing region (Fbr)	0.54359	1.06315*	0.51956	3
Fillets (F)	0.97820*	0.62854	0.34966	4
Bolt holes (Bh)	0.69950	0.90724*	0.20775	5
Bolt cover (Bc)	0.44185	1.16489*	0.72304	2
Wall thickness (Wt)	0.20732	1.39943*	1.19211	1

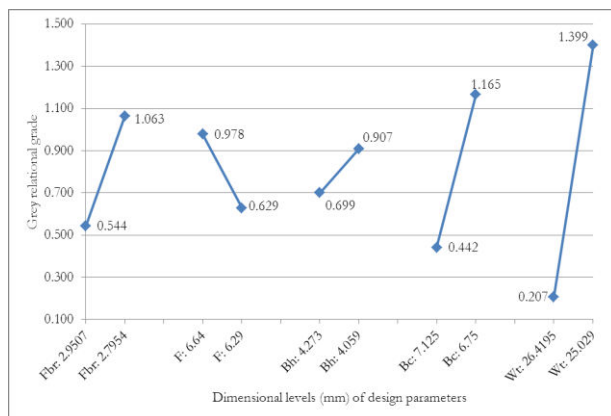


Figure-6. Effect of dimensional levels of design parameter on multi-objectives.

In the practical product design/optimization, it is so hard to find the best combination of dimensional values so as to optimize the multi objectives. Through the Taguchi method based GRA coupled with PCA, it is proved that the correlation extent can be measured between the dimensions of gear casing (design parameters) and multi objective response variables to choose the optimum setting of these design parameters. Also it can provide a quantitative measure for developing the trend of product design.

4.2.5 Confirmation analysis

Once the optimal levels of design parameters in the gear casing are identified, the conformation analysis is performed to verify the improvement on the performance characteristics. So, the linear static analysis and modal analysis using optimum levels (Fbr_{2.7954}, F_{6.64}, Bh_{4.059}, Bc_{6.75} and Wt_{25.029}) obtained by the proposed method are carried out by the following steps. Elements are translated to decrease the radius of the fillets so as to match the chosen optimum dimensional levels in each design parameter. Since all elements cannot be moved, they are moved to reduce the radius of the fillets approximately. For example, the original design value of 3.106 mm of fillet at bearing region is to be translated to optimized value of 2.7954 mm. Then the value of $3.106 - 2.7954 = 0.3106$ mm is translated by reducing the value $0.3106/2 = 0.1553$ mm on both sides so that the radius of the fillet will be equal to 2.7954 mm. This procedure is carried out using Hypermesh as preprocessor. The bolt holes are constrained to all degrees of freedoms for modal analysis. Loads are applied at four bearing regions to calculate the stiffness in turn the displacement. The modal analysis and linear static analysis are solved using Radioss solver and the results are better when compared to the base design values as shown in Tables 10 and 11.

**Table-10.** Displacement after shape optimization.

Bearing surface	Displacement (mm)	
	After shape optimization	% change from baseline values
F _x BTM	0.0745	-18.1
F _y BTM	0.0247	-34.7
F _z BTM	0.0113	-33.1
M _x BTM	0.000166	-35.9
M _y BTM	0.000526	-15.8
M _z BTM	0.00177	-17.7
F _x TOP1	0.0714	-36.8
F _y TOP1	0.0249	-34.0
F _z TOP1	0.0276	-21.4
M _x TOP1	0.000111	-49.5
M _y TOP1	0.000944	-38.3
M _z TOP1	0.002552	-1.5
F _x TOP2	0.131	-35.5
F _y TOP2	0.0255	-30.9
F _z TOP2	0.0334	-25.1
M _x TOP2	0.000116	-47.0
M _y TOP2	0.00115	-37.8
M _z TOP2	0.00166	-36.6
F _x TOP3	0.0597	-27.5
F _y TOP3	0.0254	-18.6
F _z TOP3	0.029913	-14.5
M _x TOP3	0.000118	-48.5
M _y TOP3	0.000969	-25.5
M _z TOP3	0.000763	-27.3

Table-11. Natural of frequency after shape optimization.

Mode	Natural frequency (Hz)		
	Baseline value	After shape optimization	% change
1	996	1107.89	11.2
2	1150	1398.68	21.6
3	1230	1407.24	14.4

5. CONCLUSIONS

The results of topology optimization show that the gear casing which is running good in the market has still significant room for weight reduction. The parametric shape optimization is efficiently performed with the marginal increase in natural frequencies and stiffness of the gear casing. The analysis using the multi objective Taguchi method based GRA coupled with PCA displayed the influential parameters as in the order of wall thickness,

bolt cover, fillet bearing region and fillets. From the plots for main effects, the optimum dimension in each design parameter is selected. The modal analysis and linear static analysis are solved for this optimized gear casing, and it results 21.6% increase in natural frequency and appreciable displacements range from -49.5% to -1.5% compared to the respective baseline values. The results show that the multi objective Taguchi method based GRA coupled with PCA can effectively acquire the optimal combination of design parameters and the proposed approach can be a useful tool to perform the shape optimization efficiently.

REFERENCES

- [1] Bendsoe. M.P. 1995. Optimization of structural topology, shape and material, Springer.



- [2] Bendsøe, M.P. and Sigmund. O. 2003. Topology Optimization: Theory, Methods and Applications, Springer.
- [3] Chen J., Shapiro V., Suresh K., Tsukanov I. 2006. Parametric and topological control in shape optimization, Proceedings of IDETC/CIE 2006, ASME 2006 International Design Engineering Technical Conferences and Computers and Information in Engineering Conference, September 10-13, 2006, Philadelphia, Pennsylvania, USA. 575-586.
- [4] Held. H. 2009. Shape optimization under uncertainty from a stochastic programming point of view, Vieweg+Teubner.
- [5] Allaire G. 2002. Shape optimization by the homogenization method, volume 146, Springer Verlag.
- [6] Suryatama D, Bernitsas MM, Budnick GF, Vitous WJ. 2001. Simultaneous topology and performance redesign by large admissible perturbations for automotive structural design. SAE Technical paper, 2001-01-1058.
- [7] Thomke S, Fujimoto T. 1999. Front loading problem solving: Implications for development performance and capability, Portland. Portland International Conference on Management of Engineering and Technology, PICMET. '99, 234-240.
- [8] Díaz AR, Kikuchi N. 1992. Solutions to shape and topology eigen value optimization problems using a homogenization method. International Journal for Numerical Methods in Engineering. 35(7): 1487-1502.
- [9] Ma ZD, Kikuchi N, Hagiwara I. 1993. Structural Topology and Shape Optimization for a Frequency Response Problem, Computational Mechanics. 13(3): 157-174.
- [10] Ma ZD, Kikuchi N, Cheng HC, Hagiwara I. 1995. Topological optimization Technique for free vibration problems. ASME journal of applied mechanics. 62(1): 200-207.
- [11] Cheng HC, Kikuchi N, Ma ZD. 1994. Generalized Shape/topology designs of Plate/shell structures for Eigen value optimization problems. Proceedings of ASME International mechanical Engineering congress and Exposition, PED. 68(2): 483-492.
- [12] Ma ZD, Kikuchi N, Cheng HC. 1995. Topological Design for Vibrating Structures, Computer Methods in Applied Mechanics and Engineering. 121(1): 259-280.
- [13] Krishna MM. A 2001. A methodology of Using Topology Optimization in Finite element stress analysis to reduce weight of a Structure, SAE Technical paper. 2001-01-2751.
- [14] Bendsøe MP, Kikuchi N. 1988. Generating optimal technologies in structural design using Homogenization method. Computer methods in applied mechanics and engineering. 71(2): 197-224.
- [15] Bremicker M, Chirehdast M, Kikuchi N, Papalambros PY. 1991. Integrated topology and shape optimization in structural design, Mechanics of Structures and Machines. 19(4): 551-587.
- [16] Birkett C, Ogilvie K, Song Y. 1998. Optimization Applications for Cast Structures, SAE Technical Paper 981525.
- [17] Ando K, Kanda Y, Fujita Y, Hamdi MA, Defosse H, Hald J, Mørkholt J. 2005. Analysis of High Frequency Gear Whine Noise by Using an Inverse Boundary Element Method, SAE Technical Paper 2005-01-2304.
- [18] Bernhard RJ, Huff JE. 1999. Structural-Acoustic Design at High Frequency Using the Energy Finite Element Method. Journal of Vibration and Acoustics, 121(3): 295-301.
- [19] Musser CT, Rodrigues AB. 2008. Mid-Frequency Prediction Accuracy Improvement for Fully Trimmed Vehicle using Hybrid SEA-FEA Technique, SAE Technical Paper 2008-36-0564.
- [20] Møller N, Gade S. 2003. Recent Trends in Operational Modal Analysis, SAE Technical Paper 2003-01-3757.
- [21] Jambovane SR, Kalsule DJ, Athavale SM. 2001. Validation of FE Models Using Experimental Modal Analysis, SAE Technical Paper 2001-26-0042.
- [22] Yadav V, Londhe AV, Khandait SM. 2010. Correlation of Test with CAE of Dynamic Strains on Transmission Housing for 4WD Automotive Powertrain, SAE Technical Paper 2010-01-0497.
- [23] Li R, Yang C, Lin T, Chen X, Wang L. 2004. Finite element simulation of the dynamical behavior of a



speed-increase gearbox. Journal of Materials Processing Technology 150(1): 170-174.

- [24] Ćirić-Kostić S, Ognjanović M. 2006. Excitation of modal vibrations in Housing walls, FME Transactions. 34(1): 21-28.
- [25] Inoue K, Yamanaka M, Kihara M. 2002. Optimum Stiffener Layout for the Reduction of Vibration and Noise of Gearbox Housing, Journal of Mechanical Design, Transactions of the ASME. 124(3): 518-523.
- [26] Chinnaiyan P, Jeevanantham AK. 2014. Multi-objective optimization of single point incremental sheet forming of AA5052 using Taguchi based grey relational analysis coupled with principal component analysis. International Journal Precision Engineering and Manufacturing. 15(11): 2309-2316.